A! Aalto University

Kaijalainen, Antti; Pokka, Aki-Petteri; Jaskari, Matias; Huuki, Juha; Hintsala, Tommi; Kömi, Jukka

Effect of surface characteristics on strain distribution in air- bending

Effect of surface characteristics on strain distribution in air- bending

KAIJALAINEN Antti[1,a] *, POKKA Aki-Petteri[1,b], JASKARI Matias[2,c],
HUUKI Juha[3,d], HINTSALA Tommi[1,e] and KÖMI Jukka[1,f]

[1]Materials and Mechanical Engineering, Centre for Advanced Steels Research, University of Oulu, Pentti Kaiteran katu 1, 90570 Oulu, Finland

[2]Kerttu Saalasti Institute, University of Oulu, Pajatie 5, 85500 Nivala, Finland

[3]Department of Mechanical Engineering, Aalto University, Puumiehenkuja 3, 02150 Espoo, Finland

[a]antti.kaijalainen@oulu.fi, [b]aki-petteri.pokka@oulu.fi, [c]matias.jaskari@oulu.fi, [d]juha.huuki@aalto.fi, [e]tommi.hintsala@oulu.fi, [f]jukka.komi@oulu.fi

Keywords: Roughness, Hardness, Bendability, DIC, Ultra-High Strength Steel

Abstract. This study is a continuation of previous studies; therefore, the idea is to determine the influence of surface roughness and hardness on the bendability of a UHSS grade, and it is investigated with 3-point bending tests, utilizing Digital Image Correlation (DIC) for measuring the strain distributions on the outer curvature. Investigated bending samples of a 4 mm thick commercial bainitic-martensitic steel sheet were tested in different surface conditions: (1) as-rolled, (2) dry electropolished, (3) ultrasonic burnishing and (4) a combination of dry electropolishing and ultrasonic burnishing. Ultrasonic burnishing increased the surface hardness and decreased the surface roughness. Bending results showed that smoother surface did not lead to improved bending angles and higher hardness in the subsurface decreased the bending capacity, i.e., reduced the maximum bending angle and critical strain.

Introduction

For ultra-high strength strip steels (UHSS), cold bending is the most important method of forming for applications such as containers and crane booms. Bendability is commonly determined as the minimum ratio of the punch radius to the strip thickness that the steel can tolerate without the appearance of surface defects during bending to an angle of 90º [1]. However, in this study, the bendability of a UHSS grade is investigated with 3-point bending tests, utilizing Digital Image Correlation (DIC) for measuring the strain distributions on the outer curvature [2, 3, 4, 5] and not into angle of 90°. Earlier bending studies [6, 7] have shown that strain localization is the precursor to failure in the air bending of ultrahigh-strength strip steels and shear bands have been observed to initiate at depths in the range of 1 – 6 % of the total strip thickness from the surface at angles of ~45° to the surface, i.e. in the maximum shear stress directions. Thus, it is reasonable to suppose that the near-surface properties of the strip govern the bendability.

Therefore, the ultrasonic burnishing is selected to for the surface treatment, as it strongly affects the surface quality [8], by increasing the surface hardness and decreasing the surface roughness. During the burnishing the surface layer of a workpiece plastically deforms under the combined effect of the static force created by pressing the tool onto the workpiece and the dynamic force created by the ultrasonic oscillation system [9]. Ultrasonic transducers convert high frequency electrical power into ultrasonic mechanical vibration. The equipment forges the surface of the workpiece with a hard metal point more than 20000 impacts per second. There is no removal of the material surface, unlike in grinding or polishing.

As has been shown in earlier studies [3, 10], the shot blasting affects the surface quality and decreases bendability, as well as increases the hardness at the subsurface layer. This study is a

continuation of previous studies; therefore, the main aim of the present paper is to establish an understanding of how bendability can be influenced by modifying the surface characteristics using the polishing and ultrasonic burnishing to achieve the smooth and harder surface for bending trials. The differences in the extent of multi-breakage and the bend shapes are also studied, and these observations are correlated with the findings from the bending force, strain measurements and surface roughness and hardness on the bendability of a UHSS grade.

Experimental

Investigated bending samples of 4 mm thick commercial hot-rolled bainitic-martensitic steel (0.08C-0.2Si-1.0Mn, in wt.%) were tested in different surface conditions: (1) as-rolled, (2) dry electropolished (P), (3) ultrasonic burnishing (U) and (4) a combination of dry electropolishing and ultrasonic burnishing (PU), which are seen in Fig. 1a.

Surface Treatments. Dry electropolishing was utilized using a commercial electropolishing equipment (DLyte 100 HF+). The machine is equipped with a 16-litre container which can be used to polish several samples simultaneously. Instead of liquid electrolyte typical for conventional electropolishing, polymer media containing mild acids (labelled Steel 04) was used in this study, supplied by the manufacturer. Used alternating voltage was 24 V, and maximum of 2 hours polishing time was used, until roughly 20 µm was removed from the sample surface (example of as-rolled and polished surfaces are shown in Fig. 1a).

The burnishing was performed together with the Mazak FH 480 milling center and HIQUSA ultrasonic burnishing equipment (Fig. 1b), with a wolfram-carbide ball 6 mm diameter. The used milling center table feed was 2000 mm/min and the side shift 0.025 mm, while the ultrasonic burnishing forging was performed at a frequency of 19 kHz. The spring preload was 1.0 mm for the workpiece. A cutting fluid (filtered 5 % oil-water emulsion) was used to cool the tool in the process.
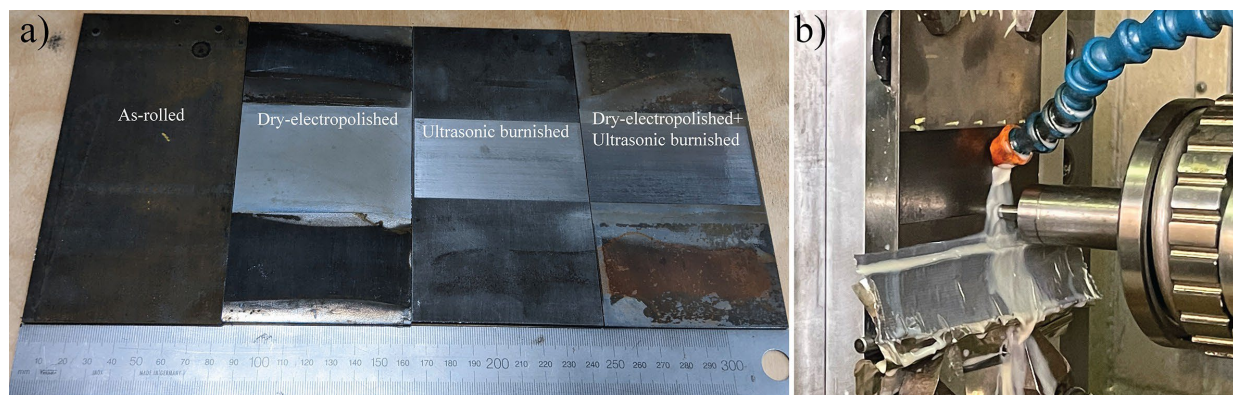

Figure 1. Setup for the burnishing equipment in the machining center.

Surface Roughness and Hardness Measurements. Surface roughness was measured using laser scanning confocal microscope (LSCM) according to ISO 4287:1997. Subsurface hardness profiles were measured using a micro-hardness tester (CSM, Switzerland) under a 0.2 (HV0.02) and 0.5 N (HV0.05) load.

Bending Trials. The investigated materials are tested in the transverse orientation, referring to the bend axis being perpendicular to the rolling direction, and they are bent until fracture. In the bending samples, the naming "b" means repeat of the test. Rectangular specimens with width (bendlength) of 80 mm and thickness of 4 mm were bent in room temperature using a Zwick 100 kN universal tensile test machine with purpose-build three-point bending tools (Fig. 2a) with DIC camera setup. The setup allows measuring of bending force, punch stroke and most importantly,

continuous DIC measurement throughout the test through the openings in the lower tool. The punch is also stationary in this setup to ensure that the measurement area stays in focus throughout the tests. As the punch is stationary, the necessary punch stroke is produced with the lower tool moving upwards at a speed of 1 mm/s. For this study, punch radius of 4 mm and a die shoulder radius of 6 mm were used, with a 70 mm gap (die width) between the centers of the shoulders. Die shoulders are freely rotating and lubricated with PTFE lubricant. More information of the test setup can be found in Refs. [2, 3].

The specimen width was chosen small enough to fit the available tools but large enough to ensure plane strain condition at the center of the bend. The bending force is expressed as force per width (N/mm) to compensate for the small variation in the specimen widths. The punch stroke data was used to calculate the bending angles throughout the test according to ISO 7438:2016. The punch stroke data was adjusted for the vertical elasticity of the setup (combined rigidity of the tensile test machine and the bending tools), measured at 51.9 kN/mm.

The DIC-system used for measuring deformation on the outer surface of the bend was Strainmaster by Lavision, equipped with two monochrome CCD cameras with a resolution of 2456 × 2058 pixels. The specimens were painted with a black-and-white speckle pattern to enable accurate tracking of points on the measured surface by the DIC-software (DaVis 8.4). The DIC recording and processing parameters are presented in Table 1. Fig. 2b provides an example of a strain map of the outer surface of a bent specimen, obtained through DIC measurement. From the obtained strain maps, the principal strain values were extracted from three lines (sections A – C) positioned at the centre of the bend at 10 mm intervals as can be seen in Fig. 2b. The peak strain ε_{b_max} at each point in time was calculated as the average of the peak values of the sections A – C.
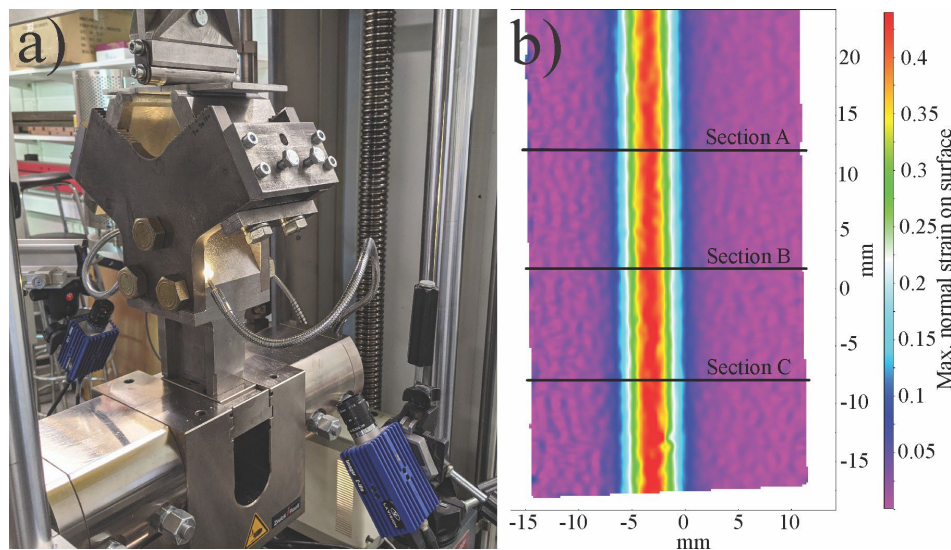

Figure 2. a) Setup for the bending tests and DIC measurements. b) Example of strain map of "Ultrasonic burnished" bend specimen at 60° angle and sections A – C.

Table 1. Recording and processing parameters for the DIC system.

DIC system and software	LaVision Strainmaster (Stereo DIC), DaVis 8.4
Sensor, digitization, imaging rate	2456 × 2058, 12-bit, 2 Hz
Lens, imaging distance, image scale	35 mm C-mount, 0.43 m, 25.7 pixels/mm
Subset size, step size, VSG	15 × 15 pixels, 5 pixels, 35 pixels
Strain window, smoothing method	5 × 5 data points, 2nd order polynomial fit
Standard deviation of principle strain	380 – 460 microstrain
Interpolation, shape function, algorithms LSM	6th order spline interpolation; affine shape function; (iterative least squares matching) algorithm based on optical flow estimation

Results and Discussion

Surface roughness and hardness. Surface roughness measurements are presented in Table 2 and roughness profiles of as-rolled, dry electropolished, ultrasonic burnishing and a combination of dry electropolishing and ultrasonic burnishing are shown in Fig. 3. R_a means the arithmetical mean deviation of the assessed profile, R_z is the maximum peak to valley height of the profile, and R_v is the max. valley depth below the mean surface. Dry electropolishing reduced the surface roughness as the R_a value decreased from 1.62 μm (as-rolled) to 0.88 μm (dry electropolished). The ultrasonic burnishing smoothed the surface even more to 0.56 μm. As previously discussed in Ref. [3, 10], R_a and R_z values might not be the most suitable values as the crack initiation during bending starts from the sharp pits or scratches, so R_v value is better to use when the correlation between the bendability and roughness is evaluated. The as-rolled material has the deepest valleys on the surface and an R_v value of 19.90 μm. While the rest of the surfaces (P, U and PU) have similar level R_v values of 3.6 – 4.6 μm.

Table 2. Investigated surface roughness values.

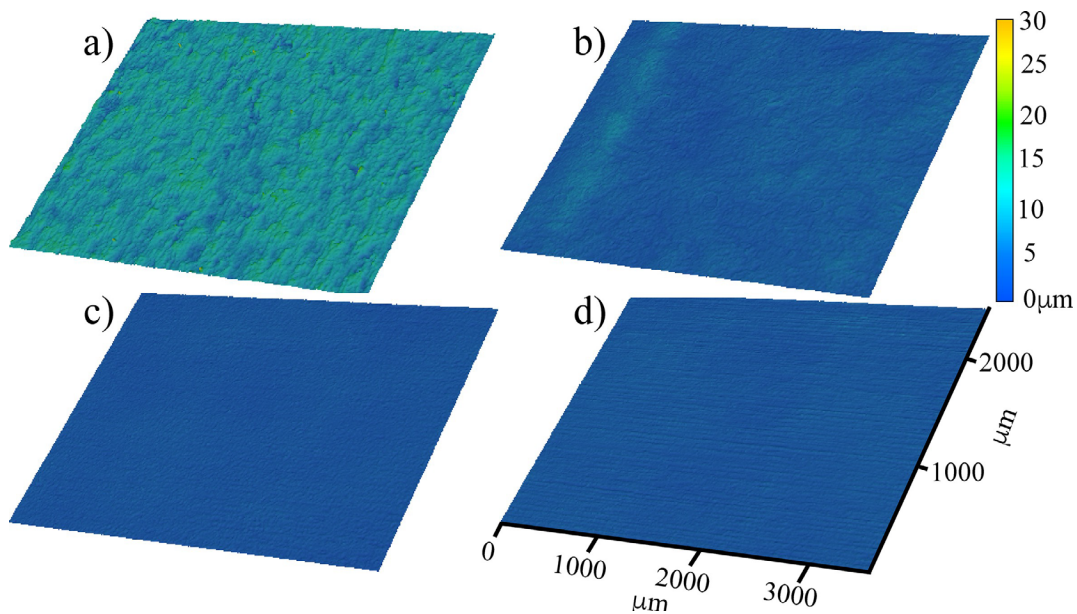| Material	R_a (μm)	R_z (μm)	R_v (μm)
As-rolled	1.62	30.30	19.90
Dry electropolished (P)	0.88	9.81	4.58
Ultrasonic burnished (U)	0.56	8.16	3.63
Polished + burnished (PU)	0.64	8.43	3.75

Figure 3. Topographical 3D surface profiles of a) as-rolled (after HCl pickling), b) dry electropolished, c) ultrasonic burnishing and d) a combination of dry electropolishing and ultrasonic burnishing.

Subsurface microhardness profiles are presented in Fig. 4. The hardnesses measured using a 200 mN load (at 25 μm below the surface) show larger scatter and higher hardness values compared to the rest of the measurements made with a 500 mN load. This means that Vickers hardness values measured using different loads are not comparable. All the samples show that the hardness generally increases throughout the thickness from the surface to 100 μm and after 100 μm the hardness is stabilized. As shown in previous studies [3, 10], the surface treatments affect the hardness values near the surface. Dry electropolishing does not seem to affect the hardness values as those are similar to the as-rolled surface hardness. However, the hardness at 25 μm below surface is increased from ~355 HV (as-rolled) to 380 HV with ultrasonic burnishing (U) or even to 405 HV with the combination of polishing and burnishing (PU). Same behavior of increased hardness is observed at 50 μm below surface. Microstructural investigation showed that the microstructure was homogenous in the measurement area.
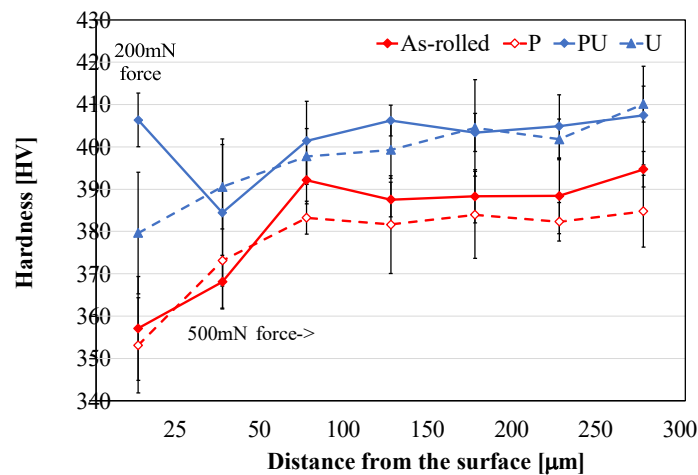

Figure 4. Hardness profiles of the investigated materials with six measurements of each. Notice: 25 μm is measured with a 200 mN load and 50 – 300 μm is measured with a 500 mN load. Therefore, the results are not comparable.

Bending. Examples of bend samples are shown in Fig. 5. The bending tests with DIC-measurement showed that the 60° bend angle is the last point where all specimens were still intact. Therefore, the strain distributions at 60° bend angle are presented in Fig. 6. The distributions were extracted from section B, illustrated in Fig. 2b. The distributions of all the specimens are almost identical at this point, and the small differences are a combination of random noise in the DIC measurement and actual variance in the material properties as seen between the as-rolled S and Sb samples (Fig. 6a) and ultrasonic burnished U and Ub samples (Fig. 6b).
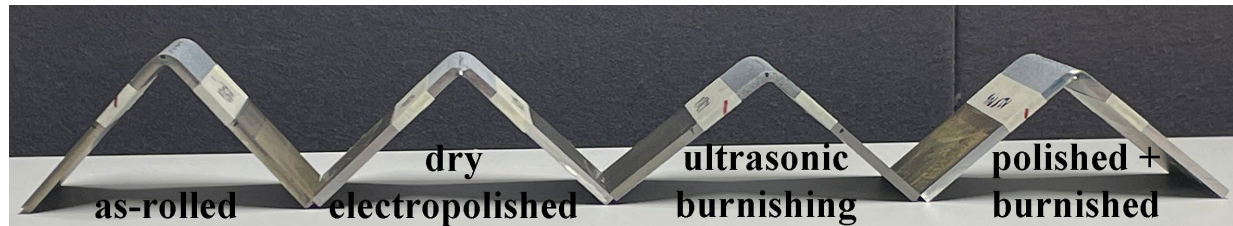

Figure 5. Examples of the bent samples with the bend axis transverse to the rolling direction.
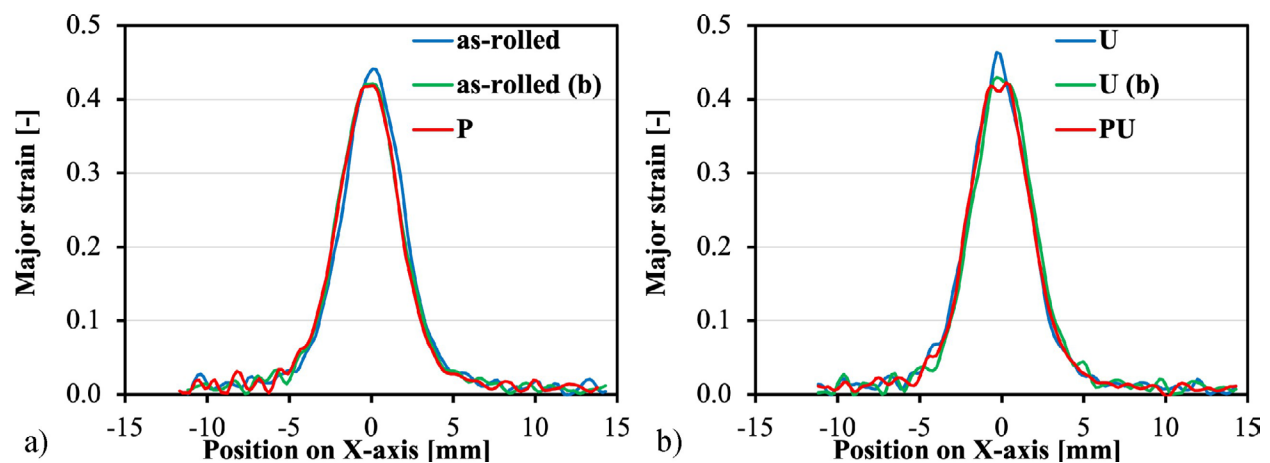

Figure 6. a, b) Strain distribution of section B of the specimens at 60° bend angle. In the bending samples, the naming "b" means repeat of the test.

The measured bending force and the average peak strain of sections A – C are plotted against the bend angle in Fig. 7. Since there were some small variations between the repeat tests of the as-rolled and ultrasonic burnished specimens, both repeats for these specimen types are included in Fig. 7. The development of both the force and the strains are near identical between all the specimens until 60° bend angle, when the first specimens start to fracture. The critical angle and strain, at which damage on the specimen surface starts to appear, can be determined from the sharp increase in the peak strain. The determined critical bending angles and peak strains of DIC-bending trials are listed in Table 3.
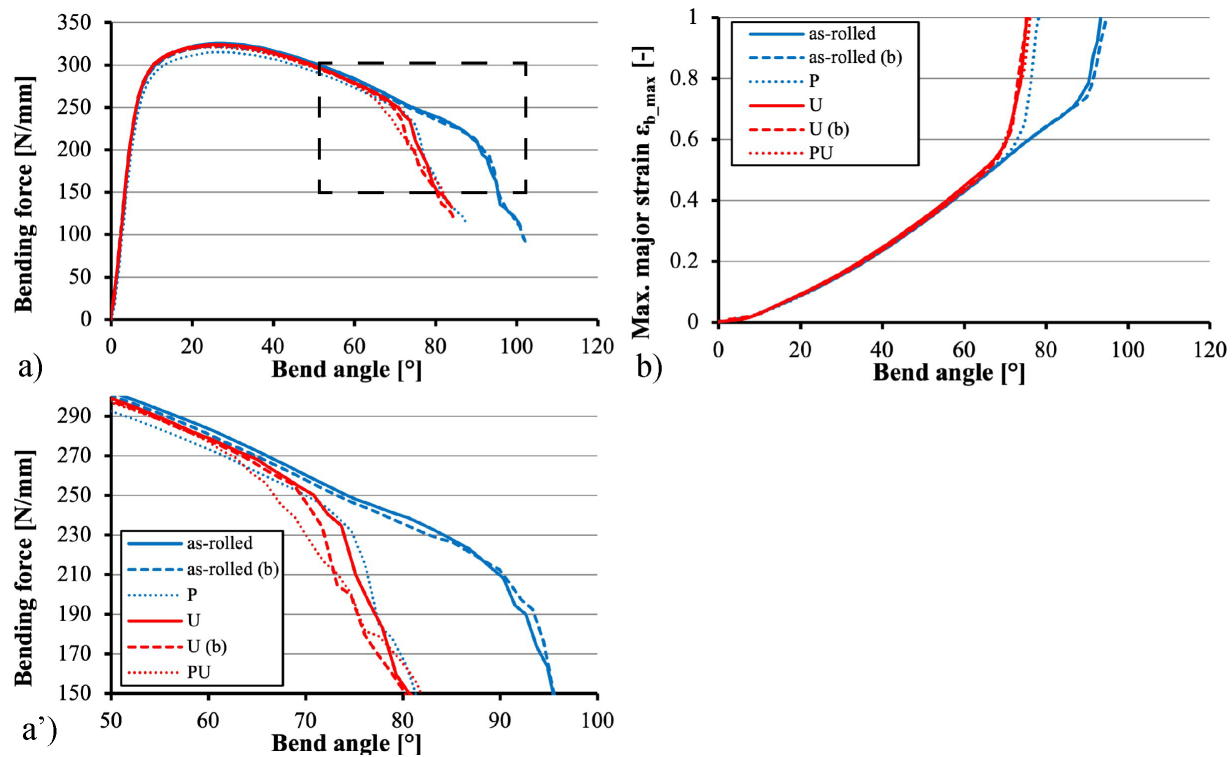
*Figure 7. Development of a) the bending force and b) the peak strain on the outside surface. a')
Magnification of bending force from bend angle 50° to 100°.*

*Table 3. Critical bending angles ($\alpha_{crit.}$) and peak strains ($\epsilon_{crit.}$) of the investigated specimens.
Results of the repeat tests in brackets.*

Material	$\alpha_{crit.}$ (°)	$E_{crit.}$ (-)
As-rolled	87 (90)	0.71 (0.74)
Dry electropolished (P)	69 (70)	0.53 (0.54)
Ultrasonic burnished (U)	65 (63)	0.50 (0.47)
Polished + burnished (PU)	66 (66)	0.50 (0.51)

Bending results showed only minor variation between repeat tests, thus it can be stated that the DIC bending test is a solid method for studying the differences between the surfaces of materials. The as-rolled tests have clearly the highest critical angle (87 – 90°) and strain (0.71 – 0.74). The polished and burnished specimens started to fracture first at approx. 65° angle or 0.50 strain. Interestingly, no major difference can be seen between the dry polished (P) and ultrasonic burnished (U or PU) samples even though the surface hardnesses were higher on the U and PU samples compared to the dry polished sample (P). Therefore, it can be stated that in this study, smoothness did not improve the bending properties and that the dry electropolishing and ultrasonic burnishing decreased the bending capacity. These treatments affect the surface, not only by increased hardness, but possibly also by increasing the dislocation densities and residual stresses. However, these factors are not determined in this study, but could be investigated in the future.

Summary

Dry electropolishing and ultrasonic burnishing were found to decrease the surface roughness. Ultrasonic burnishing increased the hardness of the surface. Both surface treatments affected the critical angle and strain significantly but had no effect on the strain distribution. Based on this, it

could be concluded that the strain distribution in bending is determined by the properties of the whole cross-section, while the critical strain is more affected by the properties near the surface. Dry electropolishing seemed to have no effect on the surface hardness, however surprisingly it still decreased the critical bending angle. The fractures may well be initiated from below the surface, in which case the surface roughness would be irrelevant. The main effect of the surface treatment (i.e., polishing or burnishing) might come from the work-hardening of the material near the surface, where the hardness is increased. Therefore, more detailed surface characterization is needed, e.g., residual stress and dislocation density investigations.

Acknowledgements

References

[1]   SFS-EN ISO 7438, Metallic materials – Bend test, (2016).

[2]   A.-P. Pokka, A.-M. Arola, A. Kaijalainen, V. Kesti, and J. Larkiola, Strain distribution during air bending of ultra-high strength steels, ESAFORM 2021, (2021). https://doi.org/10.25518/esaform21.2509

[3]   A. Kaijalainen, A.-P. Pokka, M. Jaskari, and J. Kömi, Effect of surface roughness on strain distribution during bending, IOP Conf. Ser. Mater. Sci. Eng., 1270 (2022) 012080. https://doi.org/10.1088/1757-899x/1270/1/012080

[4]   M. Kaupper and M. Merklein, Bendability of advanced high strength steels—A new evaluation procedure, CIRP Ann. Manuf. Technol., 62 (2013) 247–250. https://doi.org/10.1016/j.cirp.2013.03.049

[5]   K. Cheong, C. Butcher, and J. Dykeman, The influence of the through-thickness strain gradients on the fracture characterization of advanced high-strength steels, SAE Int. J. Mater. Manuf., 11 (2018) 2018-01–0627. https://doi.org/10.4271/2018-01-0627

[6]   A.-M. Arola, A. Kaijalainen, and V. Kesti, The effect of surface layer properties on bendability of ultra-high strength steel, AIP Conf. Proc., 1769 (2016) 200024. https://doi.org/10.1063/1.4963642

[7]   A. J. Kaijalainen, P. P. Suikkanen, L. P. Karjalainen, and D. A. Porter, Influence of subsurface microstructure on the bendability of ultrahigh-strength strip steel, Mater. Sci. Eng. A, 654 (2016) 151–160. https://doi.org/10.1016/j.msea.2015.12.030

[8]   J. Huuki, R. Ullah R, and E. Fangnon, Effects of ultrasonic burnishing on the surface quality of corrosion-resistant tool steel using a hard-carbon-coated burnishing tool, Mater. Res. Proc., 28 (2023) 1775–1780. https://doi.org/10.21741/9781644902479-192

[9]   J. Huuki and S. V. Laakso, Integrity of surfaces finished with ultrasonic burnishing, Proc. Inst. Mech. Eng. B: J. Eng. Manuf., 227 (2013) 45–53. https://doi.org/10.1177/0954405412462805

[10] A. J. Kaijalainen, V. Kesti, J. Heikkala, R. Ruoppa, D. A. Porter, and J. I. Kömi, Bendability of shot blasted ultrahigh-strength steels, Mater. Sci. Forum, 941 (2018) 510–515. https://doi.org/10.4028/www.scientific.net/MSF.941.510